A numerical solution of the NS equations based on the mean value theorem with applications to aerothermodynamics

F. Ferguson & G. Elamin
Department of Mechanical Engineering,
North Carolina A & T State University, USA

Abstract

An innovative and robust algorithm capable of solving a variety of complex fluid dynamics problems is developed. This so-called, Integro-Differential Scheme (IDS) is designed to overcome known limitations of well-established schemes. The IDS implements a smart approach in transforming 3-D computational flowfields of fluid dynamic problems into their 2-D counterparts, while preserving their physical attributes. The strength of IDS rests on the implementation of the mean value theorem to the integral form of the conservation laws. This process transforms the integral equations into a finite difference scheme that lends itself to efficient numerical implementation. Preliminary solutions generated by IDS demonstrated its accuracy in terms of its ability to capture complex flowfield behaviours. In this paper, the results obtained from the application of the IDS to two problems; namely, the hypersonic flat plate problem, and the shock/boundary layer interaction problem, are documented and discussed. In both cases, the results showed very good agreement with the physical expectation of these problems. In an effort to this new algorithm, IDS solution to the shock/boundary layer interaction problem was compared to the experimental findings described in NASA Mem., No., 2-18-59W, March, 1959. The results obtained by IDS show excellent agreement with the experimental data.

Keywords: Integro-Differential Scheme, mean value theorem, hypersonic boundary layer, finite volume, control volume, numerical scheme.

WIT Transactions on Engineering Sciences, Vol 53, © 2006 WIT Press
www.witpress.com, ISSN 1743-3533 (on-line)
doi:10.2495/HT060101

1 Introduction

The Navier-Stokes equations governing fluid flows can either be highly elliptic or highly hyperbolic, or both, depending on the applicable boundary conditions. As a result, the Navier-Stokes equations are very complicated and, in general, do not lend themselves to analytic solutions. In addition, aerospace designers are currently demanding solutions to fluid flow problems under conditions that cannot be duplicated with existing experimental facilities. Hence, the only way to obtain reasonable, complete information on fluid flows and their characteristics lies in computational fluid dynamic (CFD) methods. A literature survey indicated that there are many well-established numerical schemes available to aerospace designers. Anderson [1] and Chung [2] presented a wide variety of these schemes in their books. Akwaboa [3] used MacCormack technique to solve the supersonic flow over a rearward-facing step problem. Chang *et al.* [4], Zhang *et al*. [5] and Changh [6] introduced different versions of the space-time conservation element and solution element method for solving fluid flow problems. Even though, these schemes have led to significant improvements in the state of the art in CFD, they have many drawbacks, and therefore still not adequate to handle certain CFD demands.

1.1 Research objective

This research focuses on the development of a robust, efficient, and accurate numerical framework that is capable of solving complex fluid flow problems, and one that is capable of overcoming most of the limitations generated by existing schemes. The proposed scheme is based on a clever approach to the merging of the traditional finite volume and the finite difference schemes. In the process of creating a new numerical scheme, the mean value theorem is used to evaluate the rates of change of fluxes at the center of the control volume.

2 The governing equations

When defining any numerical solution to a fluid dynamic problem, the conservation laws must be satisfied for an appropriate set of boundary conditions. As known in fluid dynamics, the conservation laws can be applied in two basic forms; the differential form and the integral form. However, experience has shown that when the integral form of the conservation laws is applied to fluid dynamics problems, high fidelity numerical solutions can be obtained. It is therefore no surprise that the Integro-Differential Scheme (IDS) is based on the integral formulation of the conservation laws described in sub-sections 2.2, 2.2 and 2.3.

2.1 Conservation of mass equation

Consider the conservation of mass equation in the following form,

$$\oiiint_v \frac{\partial \rho}{\partial t} dv + \oiint_s \rho \overline{V} d\overline{s} = 0 \ . \tag{1}$$

In eqn (1) ρ, v, t, represent density, volume, and time, respectively. The symbols, $d\overline{s}$ and $\overline{V}$, represent the surface of the control volume and the fluid velocity, respectively. These quantities are defined through the use of the following vectors:

$$d\overline{s} = dydz\overline{i} + \quad dxdz\overline{j} + \quad dxdy\overline{k} \tag{2}$$

and

$$\overline{V} = u\,\overline{i} + \quad v\,\overline{j} + \quad w\,\overline{k} \ . \tag{3}$$

2.2 Conservation of momentum equation

Consider the conservation of momentum equation in the following form,

$$\frac{\partial}{\partial t}\oiiint_v \rho \overline{V} dv + \oiint_s \left(\rho \overline{V} . d\overline{s}\right)\overline{V} = -\oiint_s P d\,\overline{s} + \oiint_S \hat{\tau}\, d\overline{s} \tag{4}$$

where the symbol, *P,* represents pressure and the symbol, $\hat{\tau}$, is the tensor that defines the various components of the local viscous stresses. This tensor can be described by the following equation:

$$\hat{\tau} = \begin{bmatrix} \tau_{xx} & \tau_{xy} & \tau_{xz} \\ \tau_{yx} & \tau_{yy} & \tau_{yz} \\ \tau_{zx} & \tau_{zy} & \tau_{zz} \end{bmatrix} \tag{5}$$

and the symbols, $\tau_{xx}, \tau_{xy}, \tau_{yy}, \tau_{yx}, \tau_{zx}, \tau_{zy}$ and τ_{zz}, are the local shear stress components.

2.3 Conservation of energy equation

Consider the conservation of energy equation in the following form,

$$\frac{\partial}{\partial t}\oiiint_v \rho E dv + \oiint_s \rho E \overline{V} . d\overline{s} = -\oiint_s P\overline{V} . d\overline{s} + \oiint_s \hat{\tau} . \overline{V} d\overline{s} + \oiint_s \bar{\dot{q}} d\overline{s} \tag{6}$$

where the symbol, *E,* represents the total energy per unit mass of fluid. The vector, $\dot{q}$, represents the rate of heat conducted per unit area through the surface of the control volume. In general, the vector, $\dot{q}$, can be written in Cartesian coordinate format, such that

$$\bar{\dot{q}}_{vis} = \dot{q}_x\overline{i} + \dot{q}_y\overline{j} + \dot{q}_z\overline{k} \tag{7}$$

where $\dot{q}_x$, $\dot{q}_y$, and $\dot{q}_z$ represent the rate of heat conducted per unit area in *x ,y,* and *z* coordinate directions, respectively.

3 The Integro-Differential Scheme

The Integro-Differential Scheme (IDS) combines two schemes; namely, the finite volume scheme and finite difference scheme. IDS relies on the coupled behavior of discretized cells and their corresponding nodes. The numerical process is conducted in two alternating fashions, and for the sake of simplicity, only the two-dimension form of the IDS is explained in this paper. A typical control volume, illustrated in Figure 1, describes the numerical details associated with the finite volume formulation. Similarly, numerical details associated with the finite difference formulation are described through the use of Figure 2.

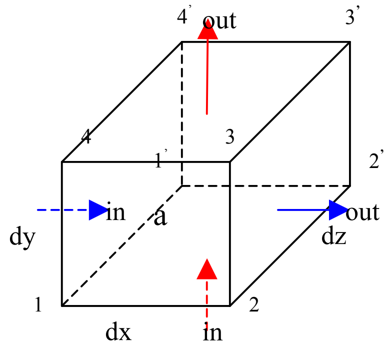

Figure 1: Finite volume model.

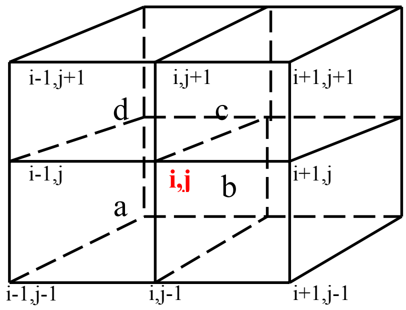

Figure 2: Finite difference model.

Moreover, as illustrated in Figure 2, the center of any four neighboring control volumes, namely, control volumes; *a, b, c,* and *d*, is defined by the indices *i* and *j*. Any control volume will be defined locally by the nodes (1, 2, 3, and 4) as shown in Figure 1, and globally by its relative location to the point *i,j* as in Figure 2.

3.1 Application of the conservation laws to the control volume

To demonstrate the utility of this numerical approach to fluid dynamic problems, consider a typical flow through the surfaces of an infinitesimal control volume, as illustrated in Figure 1. Even though the IDS has the potential to solve any 2D or 3D fluid-flow problem, for the purpose of simplicity, the discussions conducted in this paper are limited to 2D fluid flow problems. However, when describing the 2D approach, a major challenge involves the conversion of the naturally 3D conservation laws into their 2D counterparts that maintain the integrity of the 3D flowfield and its associated effects. To achieve this goal, the control volumes are chosen as infinitesimal rectangular prisms, with unit normal, **ñ**, in the *x, y,* and *z* directions. Also it was assumed that, the dimension, dz, of a typical control volume is always a single unit. These assumptions led to the fact that the fluid properties in the z-direction across any control volume are constants and the net flow of mass, momentum, and energy in the z-direction is always zero. Armed with these assumptions, the algebraic forms of the rate of change of mass, momentum, and energy at the center of each control volume are formulated as follows:

$$\left(\frac{\partial \rho}{\partial t}\right)^{average} = \left[\frac{\left((\rho u)_1 + (\rho u)_4\right) - \left((\rho u)_2 + (\rho u)_3\right)}{2\Delta x}\right] + \left[\frac{\left((\rho v)_1 + (\rho v)_2\right) - \left((\rho v)_3 + (\rho v)_4\right)}{2\Delta y}\right] \tag{8}$$

$$\begin{aligned}\left(\frac{\partial E}{\partial t}\right)^{average} = & \left[\left(\frac{(\rho Eu)_1 + (\rho Eu)_4}{2\Delta x}\right) - \left(\frac{(\rho Eu)_2 + (\rho Eu)_3}{2\Delta x}\right)\right] + \\ & \left[\left(\frac{(\rho Ev)_1 + (\rho Ev)_2}{2\Delta y}\right) - \left(\frac{(\rho Ev)_3 + (\rho Ev)_4}{2\Delta y}\right)\right] + \\ & \frac{1}{\gamma M_\infty^2}\left[\left(\frac{(\rho Tu)_1 + (\rho Tu)_4}{2\Delta x}\right) - \left(\frac{(\rho Tu)_2 + (\rho Tu)_3}{2\Delta x}\right)\right] + \\ & \frac{1}{\gamma M_\infty^2}\left[\left(\frac{(\rho Tv)_1 + (\rho Tv)_2}{2\Delta y}\right) - \left(\frac{(\rho Tv)_3 + (\rho Tv)_4}{2\Delta y}\right)\right] - \\ & \frac{1}{\mathrm{Re}_L}\left[(\tau_{xx})^{left}\left(\frac{u_2 + u_3}{2\Delta x}\right) - (\tau_{xx})^{right}\left(\frac{u_1 + u_4}{2\Delta x}\right)\right] - \\ & \frac{1}{\mathrm{Re}_L}\left[(\tau_{xy})^{lower}\left(\frac{v_3 + v_4}{2\Delta y}\right) - (\tau_{xy})^{upper}\left(\frac{v_1 + v_2}{2\Delta y}\right)\right] - \\ & \frac{1}{\mathrm{Re}_L}\left[(\tau_{yy})^{lower}\left(\frac{v_3 + v_4}{2\Delta y}\right) - (\tau_{yy})^{upper}\left(\frac{v_1 + v_2}{2\Delta y}\right)\right] - \\ & \frac{1}{\mathrm{Re}_L}\left[(\tau_{xy})^{left}\left(\frac{u_2 + u_3}{2\Delta x}\right) - (\tau_{xy})^{right}\left(\frac{u_1 + u_4}{2\Delta x}\right)\right] + \\ & \frac{1}{\mathrm{Re}_L \Pr M_\infty^2}\left[\frac{\left((\dot{q}_{xx})^{left} - (\dot{q}_{xx})^{right}\right)}{\Delta x} + \frac{\left((\dot{q}_{yy})^{lower} - (\dot{q}_{yy})^{upper}\right)}{\Delta y}\right]\end{aligned} \tag{9}$$

$$\begin{aligned}\left(\frac{\partial(\rho u)}{\partial t}\right)^{average} = & \left[\frac{\left((\rho u^2)_1 + (\rho u^2)_4\right) - \left((\rho u^2)_2 + (\rho u^2)_3\right)}{2\Delta x}\right] + \\ & \left[\frac{\left((\rho vu)_1 + (\rho vu)_2\right) - \left((\rho vu)_3 + (\rho vu)_4\right)}{2\Delta y}\right] + \\ & \frac{1}{\gamma M_\infty^2}\left[\frac{\left((\rho T)_1 + (\rho T)_4\right) - \left((\rho T)_2 + (\rho T)_3\right)}{2\Delta x}\right] - \\ & \frac{1}{\mathrm{Re}_L}\left[\frac{\left((\tau_{xx})^{left} - (\tau_{xx})^{right}\right)}{\Delta x} + \frac{\left((\tau_{xy})^{lower} - (\tau_{xx})^{upper}\right)}{\Delta y}\right]\end{aligned} \tag{10}$$

$$\begin{aligned}\left(\frac{\partial(\rho v)}{\partial t}\right)^{average} = & \left[\frac{\left((\rho v^2)_1 + (\rho v^2)_2\right) - \left((\rho v^2)_3 + (\rho v^2)_4\right)}{2\Delta y}\right] + \\ & \left[\frac{\left((\rho uv)_1 + (\rho uv)_4\right) - \left((\rho uv)_2 + (\rho uv)_3\right)}{2\Delta x}\right] + \\ & \frac{1}{\gamma M_\infty^2}\left[\frac{\left((\rho T)_1 + (\rho T)_2\right) - \left((\rho T)_3 + (\rho T)_4\right)}{2\Delta y}\right] - \\ & \frac{1}{\mathrm{Re}_L}\left[\frac{\left((\tau_{yy})^{lower} - (\tau_{yy})^{upper}\right)}{\Delta y} + \frac{\left((\tau_{xy})^{left} - (\tau_{xy})^{right}\right)}{\Delta x}\right]\end{aligned} \tag{11}$$

The non-dimensional total energy, *E,* is

$$E = \frac{T}{\gamma(\gamma - 1)M_\infty^2} + \frac{u^2 + v^2}{2}. \tag{12}$$

3.2 Flowfield Construction

A careful examination of the governing eqns (8) – (11), indicates that the system is closed relative to four unknown variables, namely ρ, u, v, and T. These unknowns are included in a solution vector, U_m, such that

$$U = \begin{bmatrix} U_1 \\ U_2 \\ U_3 \\ U_4 \end{bmatrix} = \begin{bmatrix} \rho \\ \rho u \\ \rho v \\ E \end{bmatrix} \tag{13}$$

Using Taylor's expansion, the solution can be constructed based of the following time marching scheme:

$$(U_m)_{i,j}^{t+\Delta t} = (U_m)_{i,j}^{t} + \left(\frac{dU_m}{dt}\right)_{i,j} \Delta t \,. \tag{14}$$

3.3 IDS Marching Steps

Eqn (14) represents a typical explicit time marching scheme. Like most established numerical schemes the IDS uses eqn (14). However, the major differences in the IDS as compared to the so-called established explicit schemes, is the way it handles the right side of eqn (14), namely, the old values of the solution flux vector, $(U_m)_{i,j}^t$, the time derivative vector, $(dU/dt)_{i,j}^m$, and the time step, Δt.

3.3.1 Evaluation of the time derivative

The evaluation of the time derivatives, $(dU/dt)_{i,j}^m$, , is accomplished through the use of the mass, momentum, and energy equations. Eqns (8) – (11) are implemented globally to obtain the time derivative $(dU/dt)_{i,j}^m$, at the center of each cell, *a, b, c,* and *d.* In another consistence averaging process, the time derivative at node, *(i,j),* is obtained as an arithmetic average of the time derivatives at the cell centers.

$$\left(\frac{dU_m}{dt}\right)_{i,j} = \frac{1}{4}\left[\left(\frac{dU_m}{dt}\right)_a + \left(\frac{dU_m}{dt}\right)_b + \left(\frac{dU_m}{dt}\right)_c + \left(\frac{dU_m}{dt}\right)_d\right]_{i,j} \tag{15}$$

3.3.2 Evaluation of the solution vector

As indicated in Figure 3, information at the point of interest, (i, j), is updated solely based on the values of the point in question along with all its eight immediate neighbors. All required fluxes and derivatives are evaluated based on arithmetic averages of the primitive variables.

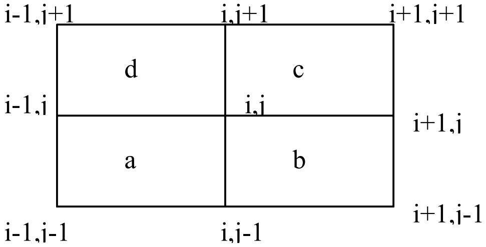

Figure 3: Illustration of the IDS stencil.

3.3.3 Evaluation of the time increment

Since the IDS is an explicit scheme, the time increment, Δt, is subject to a stability criterion. To determine the size of the time step, the Courant-Friedrichs-Lewy (CFL) criterion, documented in Anderson [1], is used.

4 Results and discussions

In this paper, the IDS is employed to solve two problems; namely, the hypersonic flat plate problem, and the shock/boundary layer interaction problem.

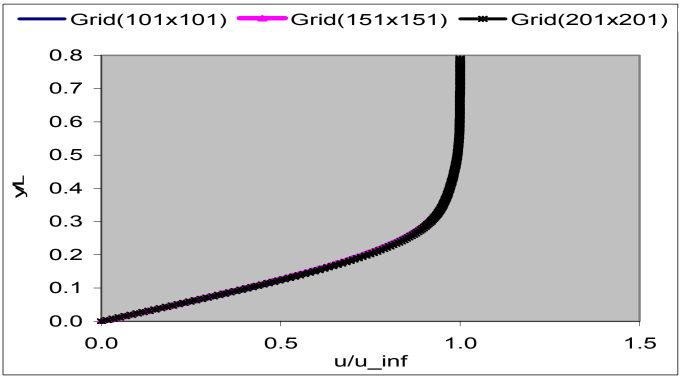

Figure 4: Grid independence studies.

4.1 The supersonic flow over a flat plate problem

The hypersonic flow over a flat plate is a classical fluid dynamics problem, and in the past it has received considerable attention [1, 3, 7]. However, it has no exact analytical solution. The IDS solver was used to solve the flat plate problem under a variety of conditions, ranging from incompressible to compressible to hypersonic. The results provided in this study are for a Reynolds Number, *Re* = 1000, and a Mach number of 4.0. The results of validation studies conducted, using grid densities and residual errors are indicated in Figures 4 and 5. Grid studies were conducted over the following grid sizes; namely, 101x101, 151x151, and 201x201. Convergence studies were conducted on a Dell, Intel based PC until residual errors were in the range of 10^{-14} – 10^{-15}. The plot in Figures 5 indicates the horizontal velocity profile obtained from the grid density studies. In Figure 6, the maximum residual obtained from the mass, momentum, and the energy fluxes is plotted as a function of the time step. To further strengthen the validity of the algorithm, the reference temperature method was used to evaluate the skin friction coefficient, C_f , and the wall heat transfer coefficient, and Stanton number, C_h (Rasmussen [8]). Data obtained from these studies were also positive.

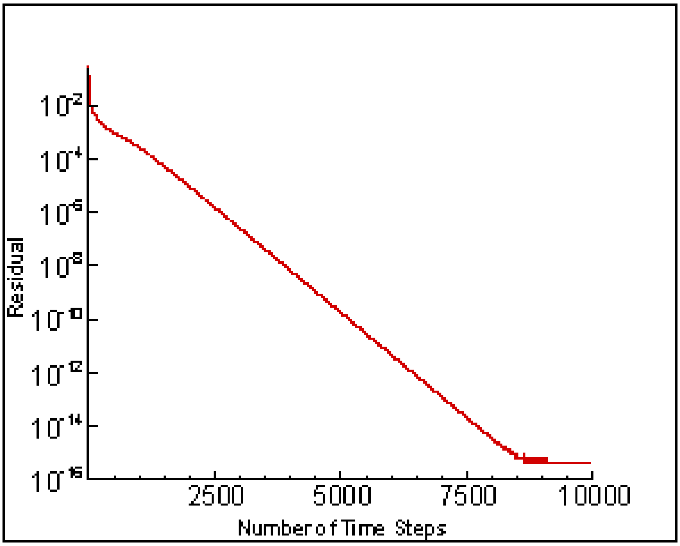

Figure 5: Residual error studies.

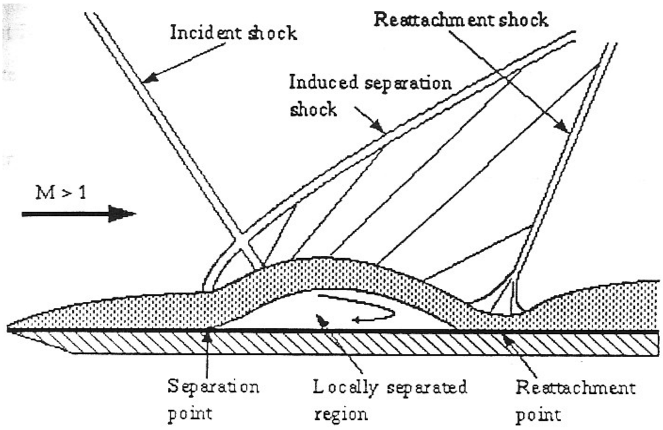

Figure 6: Illustration of the shock boundary-layer interaction problem.

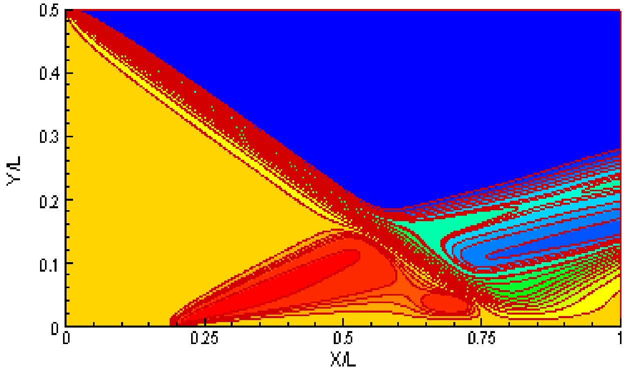

Figure 7: Illustration of IDS obtained y-velocity component distribution.

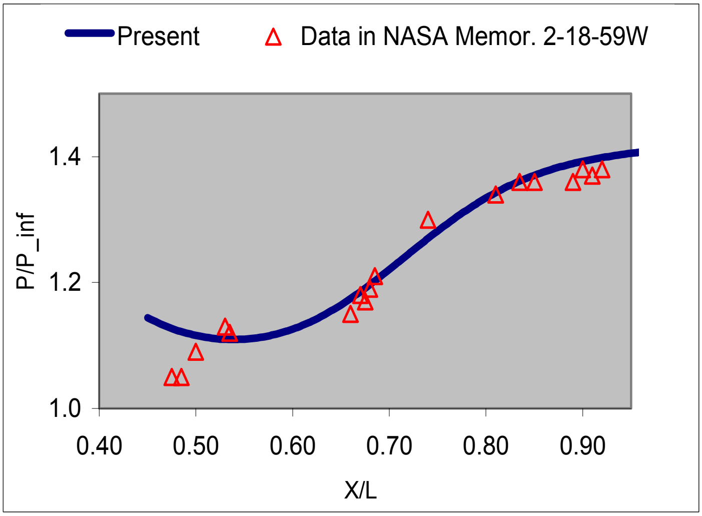

Figure 8: Pressure distribution along the wall.

4.2 The shock/boundary layer interaction problem

In 1959, Hakkinen *et al.* [9] studied the shock wave/boundary layer interaction problem experimentally. This problem is illustrated in Figure 6. More recently, due to the massive increase in computer capabilities, studies, [10, 11, 12], investigated this problem numerically. Using the IDS Solver, the inlet, outlet, and far field boundary conditions were set to be same as those of the flat plate problem. However, the flow on the top boundary is specified to form an oblique shock impinging on the wall. The bottom boundary consists of freestream and solid wall boundaries, whose lengths are 0.2 and 0.8 respectively. The flow Reynolds was set to 296000 and the Mach number set to 2.0. Figure 7 illustrates the carpet plot of the y-velocity component obtained from this study. Figures 8 and 9 compare the pressure and the friction coefficient along the solid wall with the experimental data obtained by Hakkinen *et al.* [9]. The present results are in good agreement with the experimental data.

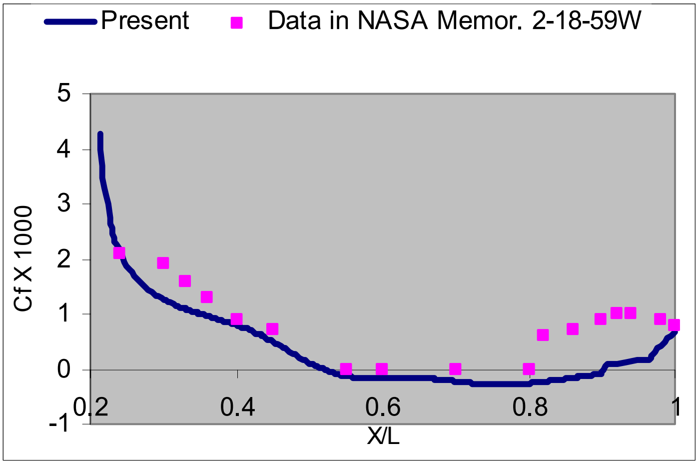

Figure 9: Skin friction distribution along the wall.

5 Conclusion

A new numerical scheme for solving equations that govern fluid dynamics problems was developed. This innovative scheme is called the 'integro-differential scheme' and abbreviated as IDS. The scheme name depicts exactly what it says, by combining the integral form of the conservation laws to formulate the governing equations and transforming them in a suitable differential form for appropriate finite difference representation. The concept of the control volume was considered when calculating the integrations and the finite difference held for the numerical implementation of the scheme. In this paper the new scheme is employed to solve the viscous flow over a flat plate problem and the shock/boundary layer interaction problem. In both cases, the results showed very good agreement with the physical expectation of the flow, the empirical formulas, and the experimental data. This agreement solidified the belief that the scheme is robust, efficient, and capable of solving a variety of complex fluid dynamics problems.

References

[1] Anderson, Jr., J. D., "Computational Fluid Dynamics-The basis with applications", McGraw-Hill, Inc., 1995.

[2] Chung, T. J., "Computational Fluid Dynamics", Cambridge University Press, 2002.
[3] Stephen Akwaboa, "Navier-Stokes Solver for a Supersonic Flow over a Rearward-Facing Step", M. S. Thesis, (Department of Mechanical Engineering, North Carolina A & T State University, Greensboro, 2004).
[4] Chang, S. C., Wang, X. Y., & Chow, C. Y., "The space-time Conservation Element and Solution Element method: A new high-resolution and genuinely multidimensional paradigm for solving conservation law", Journal of Computational Physics, Vol. 156, 1999, PP 89-136.
[5] Zeng-Chan Zhang, John Yu, S. T. & Sin-Chung. Chang, "The space-time Conservation Element and Solution Element Method for Solving the Two and Three Dimensional Unsteady Euler Equations Using Quadrilateral and Hexahedral Meshes", Journal of Computational Physics, Vol. 175, 2002, PP 168-199.
[6] Sin-Chung. Chang, "The Method of space-time Conservation Element and Solution Element- A New Approach for Solving the Navier-Stokes and Euler Equations", Journal of Computational Physics, Vol. 119, 1995, PP 295-324.
[7] MacCormack, R. W., "Current Status of Numerical Solutions of the Navier-Stokes Equations", AIAA paper no. 85-0032, 1985.
[8] Maurice Rasmussen, & David Ross Boyd, "Hypersonic flow", John Wiley & Sons Inc., 1994.
[9] Hakkinen, R. J., Greber, I., Trilling, L. & Abarbanel, S. S., "The interaction of an oblique shock wave with a laminar boundary layer.", NASA Memor. 2-18-59W, March (1959).
[10] Reyhner, T. A. , & Flugge-Lotz, I., "The interaction of a shock wave with a laminar boundary layer", Int. J. Non-linear mechanics, Vol. 3, PP. 173-199.
[11] Grasso, F., & Marini, M., "*Analysis of Hypersonic Shock-Wave Laminar Boundary-Layer Interaction Phenomena*", Computers and Fluids Journal, Vol. 25, No. 6, PP 561-581, 1996.
[12] Moujin Zhang, John Yu, S. T. , & Sin-Chang, "*Solving the Navier-Stokes Equations by the CESE Method*". AIAA paper no. 2004-0075, 2004.